J Mater Sci (2015) 50:2502–2509
DOI 10.1007/s10853-014-8808-9

Molecular dynamics of ionic self-diffusion at an MgO grain boundary

Fabio Landuzzi · Luca Pasquini · Simone Giusepponi · Massimo Celino · Amelia Montone · Pier Luca Palla · Fabrizio Cleri

Received: 17 October 2014 / Accepted: 20 December 2014 / Published online: 6 January 2015

Abstract The characterization of self-diffusion in MgO grain boundaries is a materials science problem of general interest, being relevant to the stability and reactivity of MgO layers in artificial nanostructures as well as to the understanding of mass transport and morphological evolution in polycrystalline metal oxides which are employed in many technological applications. In addition, atomic transport in MgO is a key factor to describe the rheology of the Earth's lower mantle. In this work, we tackle the problem using a classical molecular dynamics model and finite-temperature simulations. To this purpose, we first design a stable grain boundary structure, which is meant to be representative of general internal interfaces in nanocrystalline MgO. The Mg and O self-diffusion coefficients along this grain boundary are then determined as a function of temperature by calculating the mean-square ionic displacement in the boundary region. Two different diffusion regimes at low and high temperature are identified, allowing to obtain the relevant activation enthalpies for migration from the temperature dependance of the diffusion coefficients. Our results prove that Mg diffusion along MgO grain boundaries is sufficiently fast to explain the recently reported development of MgO hollow structures during repeated hydrogen sorption cycles in Mg/MgO nanoparticles.

F. Landuzzi · L. Pasquini (✉)
Department of Physics and Astronomy and CNISM, University of Bologna, v.le Berti-Pichat 6/2, 40127 Bologna, Italy
e-mail: luca.pasquini@unibo.it

S. Giusepponi · M. Celino · A. Montone
ENEA, C. R. Casaccia, Via Anguillarese 301, 00123 Roma, Italy
e-mail: massimo.celino@enea.it

P. L. Palla · F. Cleri
Institut d'Eléctronique, Microélectronique et Nanotechnologie (UMR CNRS 8520), Université de Lille I, 59652 Villeneuve d'Ascq, France

Introduction

Polycrystalline metal-oxide materials are employed in many technological applications such as structural ceramics, solid oxide fuel cells, gas sensors, thermal barrier coatings, high-Tc superconductors, and semiconductor photoanodes, just to name a few. Grain boundaries (GBs) in these materials can be both beneficial and detrimental to the desired properties and have been intensively studied [1]. In addition, the presence of GBs influences the microstructure stability during operation at elevated temperature by providing short-circuit paths for mass transport and morphological evolution via atomic diffusion [2]. In terms of GB structure and properties, the model system magnesium oxide (MgO) has been characterized by several experimental techniques [3–5] and theoretical calculations based on both interatomic potentials and density functional theory [6–9]. Measurements and theoretical calculations of atomic diffusion in MgO GBs are important in order to address materials-related phenomena spanning a huge spatial range, from the planetary size down to the nanoscale. Indeed, diffusion in MgO under high pressure (both volume and boundary) controls the rheology of the Earth's lower mantle, which contains (Mg, Fe)O ferro-periclase minerals, and therefore represents an important subject in geophysical research [9–12]. At the other extreme, the interplay between the diffusion of Mg^{2+} cations and O^{2-} anions across nm-thick MgO layers induces the formation of peculiar nano objects [13–16].

In recent experiments involving oxidation of Mg nanoparticles, a net flow of Mg vacancies toward the nanoparticle core was observed, and the proposed explanation was the faster diffusion of Mg cations with respect to O anions across the growing oxide skin. Interestingly, such a "nanoscale equivalent" of the Kirkendall effect [14] resulted in partly or completely hollow MgO cages, depending on the experimental conditions [13]. Slightly different experiments also showed the progressive development of hollow MgO structures, once Mg/MgO core/shell nanoparticles were subjected to hydrogen gas absorption/desorption cycles [15, 16]. Noteworthy, all such phenomena take place at low homologous temperatures for the MgO system, and on relatively short timescales. Under such conditions, however, lattice diffusion is not sufficiently fast to explain the formation of these exotic structures. In fact, by taking literature data for the MgO system [10, 11, 17], it can be estimated that lattice self-diffusion could not even account for Mg transport across the thin MgO shell (≈5 nm) surrounding the nanoparticles. On the other hand, since the shell generally exhibits a nanocrystalline microstructure, with grain size ≈10 nm [18], other diffusion routes can be active. In particular, GB diffusion might become possible, thanks to the high volume fraction of interfacial fast diffusion paths.

Unfortunately, only few experimental data for MgO GB self-diffusion are available to support and quantitatively check this hypothesis [12]. Therefore, a theoretical model of grain boundary structures in MgO coupled to atomistic simulations could help the understanding of the diffusion process. The atomistic simulation of diffusion in solid-state systems is complicated by the fact that it requires a very large sample, and accurate statistical analysis, to provide meaningful results; moreover, very long simulation times are required to detect the slow diffusivity of Mg. For the above reasons, a fully quantum-mechanical description of the interatomic forces and atomic dynamics is out of reach, and the empirical molecular dynamics (MD) approach seems more suitable to capture the entire physical process.

Therefore, in this study, we designed a stable MgO symmetric tilt grain boundary, characterized by a high tilt angle, and hence high excess energy, in order to be representative of the generally random grain boundaries likely present in such a constrained nanostructure [19]. In such high-angle, high-energy grain boundary, diffusion should be enhanced up to liquid-like values [20] and could be more easily detected and characterized. We directly calculate the diffusive behavior of the anion and cation as a function of temperature. Diffusion coefficients are obtained by extracting the slope of the mean-squared displacement as a function of the simulation time, by averaging over a number of diffusing ions in the GB plane, and over a number of similar MD simulations. At variance with the only previous studies [6, 7], which focused on the diffusive behavior of single Mg and O ions within a frozen structure, by looking at the profile of the migration barriers at vanishing temperature, in the present work we attempted to characterize the self-diffusion by direct simulations of all the active degrees of freedom, as a function of temperature. The obvious disadvantage of such a direct approach is the much longer computer simulation times, due to the fact that the diffusion barriers are much higher than the thermal energy available at any temperature. However, the quality of the statistical sampling of the diffusion paths, and therefore of the results, is also considerably improved.

Computational methods

Magnesium oxide has a rocksalt lattice structure, bound by ionic attraction between the Mg^{2+} cation and the O^{2-} anion. The description of the atomic interactions in oxide crystals such as MgO, by means of empirical forces derived from a potential function, can be performed at two different levels of sophistication: (a) by a rigid-ion model, in which a formal charge is assigned to each ion and the polarization of the ions is completely neglected; or (b) by the so-called "shell" model, in which each atom is described by a negatively charged spherical shell, which can be displaced with respect to a positively charged core [21–23]. In practical terms, the rigid-ion model describes the ions as simple point-like charges bound together by electrostatic attraction. On the other hand, the shell model can describe to a good extent the ion polarization by introducing a shell representing the electronic cloud, dynamically linked to the positive ion core by a harmonic spring potential. In MgO, the cation polarization is small enough to be neglected, and therefore the Mg ion is described as rigid in both models.

Electrostatic interactions between ions, in either model, are described by a infinitely ranged $1/r$ Coulombic term, with formal charges of $+2$ and -2, respectively, for Mg and O ions. The use of formal ionic charges has been already shown to represent correctly the dynamic features of atoms in most oxide compounds. Here, we used the Ewald summation technique to compute the conditionally convergent Madelung sum (although in recent years other techniques have demonstrated comparable levels of numerical accuracy while potentially offering a better efficiency), by setting the real space cut-off value at $r_c = 5.5$ Å and a relative error on the Coulomb sum (real plus reciprocal space part) less than 10^{-5}.

Short-range repulsion was described by a Buckingham pair potential [24]:

$$V_{ij}^{\text{buck}}(r_{ij}) = A_{ij}\exp\left(-\frac{r_{ij}}{\rho_{ij}}\right) - \frac{C_{ij}}{r_{ij}^6}, \quad (1)$$

where r_{ij} is the distance between the atoms i and j, and A_{ij}, ρ_{ij}, and C_{ij} are potential parameters specific to each ion pair. The cut-off for the Buckingham potential was set to 5.5 Å. In Table 1, we report the parametrization of the potential [25]. Notice that if the electronic spring-like interaction is taken into account (shell model), the parameters change with respect to the rigid-ion model. Indeed, in the rigid-ion model, the Mg–O interaction parameter takes also into account the dipole effect due to the charge distribution around the ions. In the case of the shell model, a fractional mass equal to 0.20 atomic mass units was assigned to the shell, while the core–shell spring harmonic constant k was set to 15.74 eV/Å^2.

To assess the reliability of the two models, we computed some structural properties of a bulk MgO crystal of 8000 atoms in the rocksalt structure. Classical MD simulations at constant temperature and pressure (or {NPT}-ensemble) with the above interaction potentials were carried out with the MD code DL_POLY4 [26–28]. All MD simulations were performed using periodic boundary conditions to represent an infinite system. The bulk modulus, at $T = 0$ K, was obtained by fitting the energy versus volume curve, for different values of the anion–cation distance. The lattice parameter a_0 at $T = 0$ K was derived by minimizing the crystal potential energy. The volume as a function of temperature at zero pressure was obtained by averaging {NPT} runs over 50 ps of MD simulation. By fitting the V versus T curve, we also obtained the thermal expansion coefficient λ. Table 2 shows a comparison between theoretical values of the above quantities, obtained with both potential models, and the corresponding experimental values, where available. It can be seen that, as far as basic bulk properties are considered, there is no significant quantitative improvement in using the shell model above the rigid-ion model, since the errors on the computed quantities are of the same order of magnitude. Therefore, we decided to retain the rigid-ion model in the foregoing MD simulations of GB diffusion since, on the contrary, the computational cost of shell model MD simulations is much larger than that for the rigid-ion model.

Table 1 Parameters for the Buckingham interatomic potential [25]

	A	ρ	C
Shell model			
Mg–O	821.60	0.3248	0.00
O–O	22764.0	0.1490	20.37
Rigid-ion model			
Mg–O	1295.55	0.3000	0.00
O–O	22764.0	0.1490	27.88

In the case of shell model, shell fractional mass and core–shell spring harmonic constant $k$are also used: 0.20 and 15.74, respectively. Numerical values are expressed in native DlPoly units

Table 2 Calculated values of lattice parameter a_0, density δ, bulk modulus B, and thermal expansion coefficient λ, for bulk MgO in the rocksalt structure

	a_0 (Å)	δ (g/cm^3)	B (GPa)	λ_m (K^{-1})
Expt.	4.21	3.51	160.3	1.340E-5
Rigid ion	4.21	3.55	231.5	9.330E-6
Shell mod.	4.22	3.52	194.4	9.497E-6

In the following, the atomic system containing the grain boundary structure is described. The entire system was composed by 154000 Mg and O ions. To mimic an infinite system, periodic boundary conditions were applied in all directions. The atomic mass of both elements were fixed to their experimental values. Nosé–Hoover thermostats were used to perform MD simulations at constant temperature and constant pressure. A 1 fs time step was largely sufficient to integrate the equations of motions during the ion diffusion (with energy conservation better than $\Delta E/E \leq 10^{-5}$), even at the higher temperatures.

Grain boundary structure

Our goal was to determine whether diffusion of Mg along MgO grain boundaries is sufficiently fast to explain the formation of hollow MgO structures during hydrogen sorption cycles in Mg-based materials [15]. The nanocrystalline shell should likely include a range of many different GBs, with values of the inclination and tilt angles rather randomly distributed. Since the nanostructure is not annealed, it is likely that a large fraction of such GBs would be of high angle, and with a large excess energy stored because of the accumulation of interfacial stress [29, 30]. Therefore, we adopted a single high-angle symmetric tilt grain boundary (STGB) around the [110] polar axis, as being representative of the variety of typical internal interfaces in nanocrystalline MgO. It is worth noting that in MgO, the [110] symmetric tilt GBs are observed to be the majority of low-angle misorientations, while at larger misorientations, random asymmetric GBs are more often observed, with one of the planes being {100} [31].

As shown in Fig. 1, we built a (113)(113) STGB in the rocksalt structure, obtained by rotating one half of an MgO bulk crystal by 180 ° about the [113] direction (here taken as the z axis of the computational supercell); the x axis is parallel to a $[1\bar{1}0]$ direction, and the y axis to a $[33\bar{2}]$ direction. Note that the same STGB can be equivalently obtained by symmetrically tilting the two halves of the crystal by $\theta = \pm 70.53$ ° about the $[1\bar{1}0]$ axis. However, the

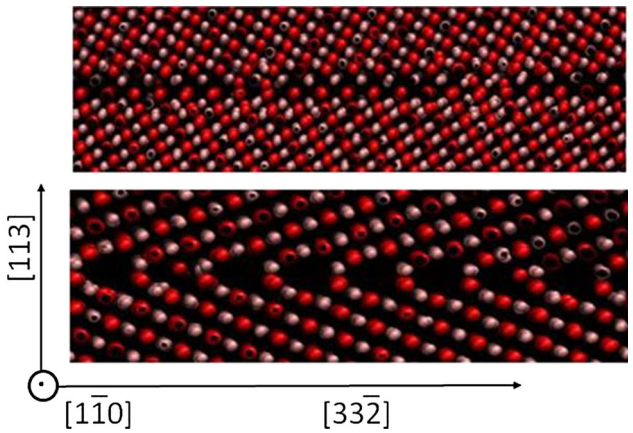

Fig. 1 Groove structure of the (113)(113) symmetric tilt grain boundary after the equilibration at $T = 300$ K. Schematic of the interface in the *xz* plane (*top*) and *yz* plane (*bottom*); *red spheres* are oxygen anions, *white spheres* are magnesium cations. The crystallographic directions corresponding to the *x*, *y*, and *z* axes are indicated with reference to the *bottom* image (Color figure online)

exact symmetrical cut of the crystal at a {113} plane, followed by a rotation as described, would bring two Mg planes immediately in contact, with the result of a strong Coulomb repulsion which would destabilize the structure. Therefore, one Mg plane was removed from one of the two half-crystals, in such a way that the GB plane could be formed by two planes of opposite charge.

Due to the periodic boundary conditions, two (initially identical) STGBs were obtained. The GB area was $A = 7382.972$ Å^2, and the total length along z was $L_Z = 200.140$ Å. The number of ions in the region about the GB plane, and potentially involved in the diffusion process, was about 5500. The GB supercell was first equilibrated at room temperature $T = 300$ K and atmospheric pressure, $P = 1$ atm., for 500 ps. Subsequently, at each temperature of study, the system was equilibrated for at least 0.5 ns, and all the physical quantities were computed by averaging over the next 0.1 ns (10^5 MD time steps).

Results and discussions

The interface region has a density lower than the bulk system and therefore diffusion should be favored in the GB plane. As it can be seen in Fig. 1, the ordered structure of the GB covers 4–6 atomic planes, and is characterized by the presence of widely spaced major grooves along the *x* direction, and of tighter and smaller (minor) grooves along the *y* direction. The atomic structure of the opposite charged planes of the present GB is not qualitatively different from the wide-grooved structure of the ab initio study by McKenna and Shluger of a (310)(310) tilt GB about the [100] axis [8]. We performed a series of relaxations at $T = 0$ K, starting from the ordered geometric structure and translating the GB in the *xy* plane by fractions of the planar unit cell while simultaneously allowing the *z* displacement to minimize the excess energy. Although non-exhaustive, this limited search for the energy minimum confirmed that, similar to the study in Ref. [8], no translation should exist in the GB plane. The calculated GB excess energy per unit area is $E_{GB} = 2.14$ J/m^2, similar to the 1.95 J/m^2 of that study.

During the finite-temperature equilibration, some defects were formed due to the energy release and the consequent increase of temperature in the region near the interface. Such defects were ions (cations or anions) that, attracted by the oppositely charged surface, moved in the middle of the groove close to the oppositely charged ion, and deformed the lattice structure around their neighbors.

We observed the motion of a single Mg cation in the interface plane, to understand which kind of diffusive events drive the ions in that region. The simulation was performed under constant-(NΣT) conditions, in which the Σ_{zz} component of the stress tensor perpendicular to the GB plane is unconstrained, and permits the system relaxation along the *z* axis under constant $\Sigma_{zz} = 0$ stress and constant temperature T. Even after quite long MD simulations, the very low diffusivity allowed to observe only a few jumps of the Mg cation between neighbor sites in the groove. Figure 2 shows a plot of the trajectory of the Mg atom over a time of 0.5 ns, jumping across four neighboring major grooves along *x* (horizontal direction in the figure), and just one jump across the minor grooves along *y*.

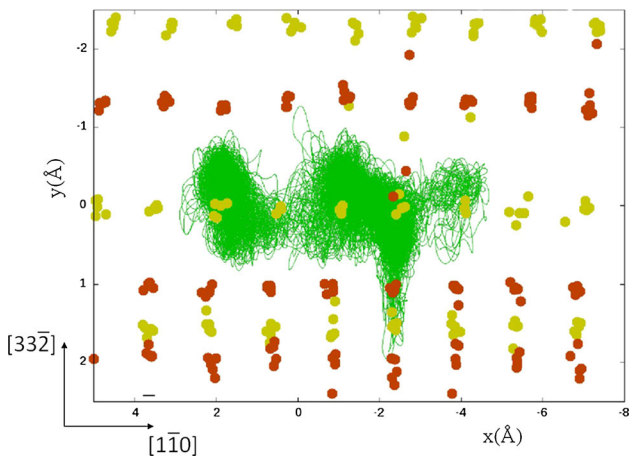

Fig. 2 Magnesium trajectory at the MgO interface in a (NΣT) ensemble ($T = 2500$ K). The trajectory of the cation (*green*) moves along the groove (*x* direction) near to the anion (*yellow dot*). In the picture, some defects are visible in the first interface layer (Color figure online)

The Mg and O diffusion coefficient D at each temperature was determined from the time evolution of the mean-squared displacement (MSD), using the Einstein relation:

$$\lim_{t\to\infty}\langle(x(t)-x_0)^2\rangle = 6Dt\,, \tag{2}$$

where the $\langle\ldots\rangle$ means ensemble averaging, and the limit to infinite time is to be intended as the extrapolation of the straight slope of the MSD plotted versus t. Note that we retain the factor 6 (bulk) instead of 4 (surface diffusion), since in the following the possibility of atoms diffusing from the GB into the bulk will also be considered.

The classical MD approach also allowed us to study how the diffusivity varies as a function of the distance from the interface plane, by tracking the MSD for ions belonging to different planes parallel to the GB. Such observation can be linked to different regimes, according to Harrison's classification of diffusion in grain boundaries [32]. The ensemble average was calculated only for ions inside a volume $V_i = \{\mathbf{x} = (x, y, z) |\, ia_0/2 \le |z| < (i+1)a_0/2\}$, where $z = 0$ identifies the interface plane.

Since the mobility of the ions is very low in the oxide, and given that the MgO melting temperature is very high ($T \approx 3125$ K), we could safely increase the temperature to get a good estimate of the diffusivity while still remaining sufficiently far from melting, over a range of temperatures spanning from 750 to 2250 K. In Fig. 3, the behavior of the MSD as a function of time for different temperatures is reported. The different lines in each figure give the MSD separately for Mg and O ions in the two volumes V_0 and V_1.

As stated above, the GB plane contains about 5500 ions, half Mg and half O. At $T = 750$ K, all MSD curves are nearly flat, corresponding to a diffusion coefficient $D < 10^{-14}$ m^2/s, which is the lower limit to detect atomic displacements (above the thermal noise) in an MD simulation of about 1 ns duration. As expected, with increasing temperature, the mobility increases progressively. At $T =$ 1000 K, it is already possible to determine a diffusion coefficient for Mg and O ions located in volume V_0, i.e., having $|z| \le a_0/2$, while the mobility remains below the thermal noise for atoms lying above or below the GB plane. At $T \ge$ 2000 K, mobility of Mg and O ions can be detected also in the region V_1, i.e., where $a_0/2 \le |z| < a_0$ from the GB plane.

As expected, Fig. 3 shows that the slope of the MSD versus time curves, proportional to the diffusion coefficient D, increases with temperature and decreases with increasing distance from the GB plane. The comparison between the two ionic species reveals that Mg and O ions exhibit a quite similar MSD versus time up to 1750 K, while at higher temperatures O becomes progressively more mobile. As seen in Fig. 3, the MSD of O anions is larger than that of Mg cations by a factor of ≈ 2 and ≈ 8 at $T = 2000$ and 2250 K, respectively. Furthermore, at $T = 2250$ K, the MSD of O anions in region V_1, i.e., at larger distance from the GB plane, can be detected by MD simulations and becomes larger than that of Mg cations in region V_0 about the GB plane.

The diffusion coefficient for both ions as a function of temperature was calculated through a linear fit of the MSD versus time curve, excluding the initial 5 ps of the MD simulation. The results obtained for the atoms in V_0 (closer to the GB plane, the only ones for which a reliable temperature dependence could be determined) are displayed in Fig. 4. The temperature dependence of D suggests the presence of two different regimes at low and high temperature. The Arrhenius fit according to $D = D_0 \exp(-E/k_BT)$ is reported in Fig. 4 separately for the low (dashed line)- and high (dotted line)-temperature regimes. At low temperature, the fits yield the following activation enthalpies for migration: $H^m_{\mathrm{Mg}} = (0.57 \pm 0.10)$ eV and $H^m_{\mathrm{O}} = (0.49 \pm 0.12)$ eV. At high temperature, the fit results are $H^m_{\mathrm{Mg}} = (1.25 \pm 0.15)$ eV and $H^m_{\mathrm{O}} = (3.3 \pm 0.6)$ eV (see equations in Fig. 4). These activation enthalpies should be compared to literature data for lattice and GB migration in MgO, a compilation of which is reported in Table 3.

The migration enthalpies for Mg and O obtained by our MD simulations in the low temperature range are very close each other, suggesting that the two ions diffuse along the same channel and experience similar jump barriers. The values are significantly lower than $\approx$1 eV reported by Harris et al. for both ions [6, 7]. Such a finding is consistent with the fact that in Harris et al.'s simulations, the activation energies were determined from the trajectory of one single ion, while the surrounding ones are frozen in their "stable" position during its motion. The coordinated motion of ions around the diffusing ones represents one improvement of our direct simulation method.

In the high-temperature regime, our results show that the migration enthalpies of the two ions differ significantly. The one for O is compatible, within the uncertainty, with the 2.0–2.7 eV range determined both theoretically and experimentally for O migration in bulk MgO, as reported in Table 3. Differently, the one for Mg is about one half of the typical values of 2.0–2.5 eV for Mg migration in bulk MgO (Table 3). Although these estimates suffer from a rather large uncertainty due to the restricted temperature range, it may be suggested that, at elevated temperatures, diffusion paths involving jumps into bulk-like sites become operative. The increase of the oxygen MSD to clearly non-zero values also in region V_1 at high temperature supports this hypothesis. The high migration enthalpy for O can be explained assuming that jumps to/from bulk-like sites

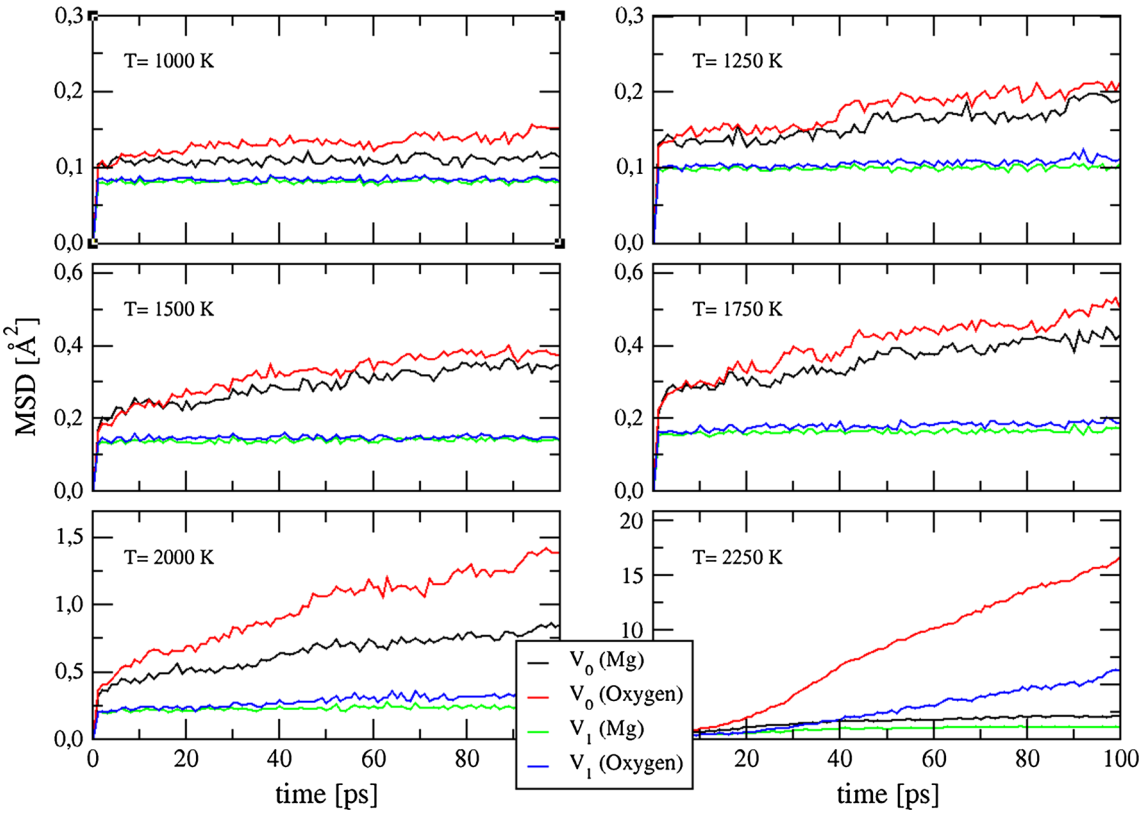

Fig. 3 Mean-squared displacements (in Å^2) of ions averaged over volumes located at different distances from the interface plane: V_0 and V_1 are volumes at short and long distances from the interface, respectively (Color figure online)

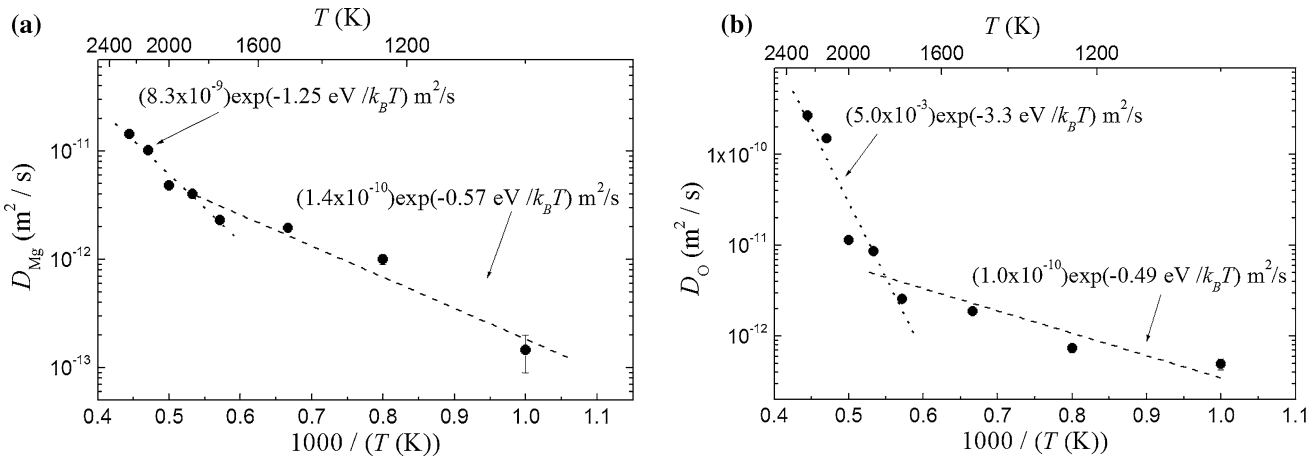

Fig. 4 Diffusion coefficient D as a function of temperature for (**a**) Mg and (**b**) O ions initially located in region V_0 close to the GB. The *lines* represent Arrhenius-like fits yielding the displayed equations for the temperature dependence $D(T)$

represent the rate-limiting step of most diffusion paths responsible for the strongly enhanced mobility of O anions. In the case of Mg, it may be speculated that only a fraction of diffusion paths involve jumps to/from bulk-like sites, resulting in a migration enthalpy which is intermediate between the ones for lattice and GB migration.

Assuming that the low temperature dependence of $D_{\mathrm{Mg}}(T)$ can be extrapolated to $T \approx 573K$, we will now estimate the time needed for the formation of MgO hollow shells when Mg/MgO core/shell nanoparticles undergo repeated hydrogen sorption cycles or are exposed to high vacuum. Figure 5 depicts schematically the relevant

Table 3 Literature data, compared to the results of this work, for Mg and O diffusion parameters in MgO lattice and GB

Parameter	Value	Exp/Theo	References
Lattice (eV)			
H^m_{Mg}	1.99	Theo	[10]
H^m_{Mg}	2.50(7)	Theo	[11]
H^m_{Ca}	2.52	Exp	[17]
H^m_O	2.00	Theo	[10]
H^m_O	2.70(8)	Theo	[11]
H^m_O	2.66	Exp	[17]
Grain boundary			
H^m_{Mg}	1.05 eV	Theo[a]	[6]
H^m_O	1.01 eV	Theo[a]	[6]
H^m_{Mg}	0.57(10) eV	Theo	This work
H^m_O	0.49(12) eV	Theo	This work
D_{Mg} (2273 K)	$\approx 10^{-7}$ m^2/s	Exp[b]	[12]
D_O (2273 K)	$\approx 5 \times 10^{-7}$ m^2/s	Exp[b]	[12]

H^m_X: migration enthalpy of X ions; $D_X(T)$: diffusion coefficient of X ions at temperature T. Exp/Theo indicates if the values are obtained by experiments or theoretical calculations, respectively

[a] Lowest value among different paths

[b] Extrapolated to 0 GPa from high-pressure data at 15 and 25 GPa

$$D^{eff}_{Mg} = D^{XL}_{Mg} + \frac{\delta^B}{d_G} D_{Mg} \approx \frac{\delta^B}{d_G} D_{Mg}$$

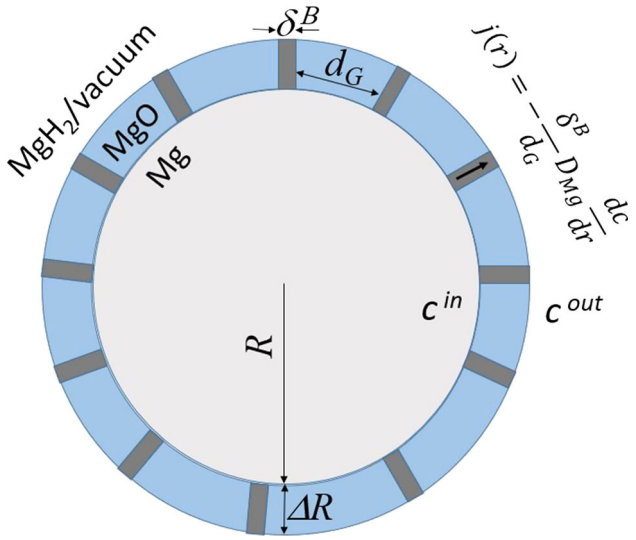

Fig. 5 Schematic representation of an Mg/MgO core/shell nanoparticle with a nanocrystalline shell. The GBs are depicted in *dark gray*. The key morphological/phase parameters and the main equations used to model outward Mg diffusion and formation of hollow structures are reported (see text for detailed explanation)

geometric parameters: for simplicity, the Mg core is represented as a sphere of radius R, and MgO as a spherical shell with thickness ΔR, average grain size d_G, and typical GB width δ^B. The effective Mg diffusion coefficient in MgO, which in general can be expressed as a combination of self-diffusivities in the lattice (D^{XL}_{Mg}) and along GBs (denoted here simply as D_{Mg}), reduces to $(\delta^B/d_G)D_{Mg}$ because lattice self-diffusion in MgO can be neglected at these temperatures. The radial outward diffusion flux can be shown to depend on the core/shell geometry and on Mg concentrations (number of atoms per unit volume) inside (c^{in}) and outside (c^{out}) the shell, according to [33]:

$$j(r) = \frac{\delta^B D_{Mg}(c^{in} - c^{out})}{d_G \Delta R} \frac{(R + \Delta R)R}{r^2}. \quad (3)$$

The inner concentration is taken as the one of bulk Mg, i.e. $c^{in} \approx 4.3 \times 10^{28}$ atoms m^{-3}, simply calculated using mass density and molar weight data. For the outer concentration, two cases shall be distinguished: during hydrogen absorption cycles, the outer material quickly transforms into magnesium hydride MgH_2, resulting in $c^{out} \approx 0.77c^{in}$ on account of the different density and molar weight of the metal and the hydride. Differently, when the nanoparticles are exposed to high vacuum, Mg atoms that reach the outer shell surface evaporate quickly due to the high vapor pressure of Mg, allowing us to assume that $c^{out} \approx 0$. Finally, the time τ such that the integrated total flux of Mg atoms across the shell equals the initial number of Mg atoms in the core can be derived from the equality: $j(R)4\pi R^2\tau = (4\pi/3)R^3c^{in}$, yielding

$$\tau \approx \frac{R^2 c^{in} \Delta R d_G}{3\delta^B D_{Mg}(c^{in} - c^{out})(R + \Delta R)} \quad (4)$$

taking $R \approx 200$ nm, $\delta^B \approx 1$ nm, $d_G \approx 10$ nm, $\Delta R \approx 5$ nm [15, 18], and $D_{Mg}(573\text{ K}) \approx 1.3 \times 10^{-15}$ m^2 s^{-1} (as derived from extrapolation of low-temperature diffusivity), we obtain a rather short time $\tau \approx 11$ s for the case of hydrogen absorption (or $\tau \approx 2.5$ s for high vacuum exposure). Even if this simple estimate pertains to a specific GB with rather wide channels, such a result indicates that, in Mg/MgO core/shell nanoparticles, appreciable Mg transport from Mg cores toward the MgO shell's outer surface may occur via diffusion along MgO GBs of the nanocrystalline shell at experimental hydrogen sorption temperatures, thus providing a possible explanation for the observed formation of MgO hollow structures [15, 16].

Conclusions

By using a rigid-ion model of the atomic interaction in MgO, we built a high-angle GB, representative of typical high-energy, constrained interfaces which are likely encountered in nanocrystalline MgO. Classical molecular dynamics simulations with a simple potential model,

including Coulomb interaction between formal charges plus a soft core short-range repulsion, were carried out over a range of temperatures, to investigate the diffusivity of Mg and O in and around the GB plane. The GB exhibits two sets of grooves along perpendicular directions, with one set being more open and widely spaced and the other being thinner and more densely packed. Ionic diffusion in and along such grooves is largely enhanced with respect to the bulk values. By studying the MSD averaged over regions located at different distances from the GB, we determined the diffusion coefficient and obtained activation enthalpies for anion and cation migration. Two different diffusion regimes were identified at low and high temperature, the former being characterized by low activation enthalpies which suggest a coordinated motion of ions around the diffusing one. In the high-temperature regime, O anions are significantly more mobile than Mg cations, and the high activation enthalpies for their motion indicate that atomic jumps into bulk-like sites are permitted. The extrapolation of Mg diffusivities down to temperatures typical for hydrogen sorption cycles in Mg-based materials shows that Mg diffusion along MgO GBs in Mg/MgO core/shell nanoparticles may lead to the formation of MgO hollow shells as recently observed experimentally.

Acknowledgements Computational resources and technical support have been provided by the CRESCO ENEA-GRID High-Performance Computing infrastructure and staff. CRESCO is funded by ENEA and by national and European research programs. Additional computational resources were provided by EDARI/CINES Montpellier, under contract x2014077225 (Nanomaterials for Hydrogen storage) to FC. We gratefully acknowledge partial financial support by the COST Action MP1103 "Nanostructured materials for solid-state hydrogen storage." FL thanks the kind hospitality of IEMN-CNRS and partial support for extended visits.

References

1. Sutton AP, Balluffi RW (1995) Interfaces in crystalline materials. Oxford University Press, New York
2. Harding JH (2003) Short-circuit diffusion in ceramics. Interface Sci 11:81–90
3. Yan Y, Chisholm MF, Duscher G, Maiti A, Pennycook SJ, Pantelides ST (1998) Atomic structure of a Ca-doped [001] tilt grain boundary in MgO. Phys Rev Lett 81:3675–3678
4. Wynblatt P, Rohrer GS, Papillon F (2003) Grain boundary segregation in oxide ceramics. J Eur Ceram Soc 23:2841–2848
5. Osenbach JW, Stubican VS (1983) Grain-boundary diffusion of 51Cr in MgO and Cr-doped MgO. J Am Ceram Soc 66:191–195
6. Harris DJ, Watson GW, Parker SC (1997) Vacancy migration at the {410}/[001] symmetric tilt grain boundary of MgO: an atomistic simulation study. Phys Rev B 56:11477–11484
7. Harris DJ, Watson GW, Parker SC (2001) Atomistic simulation studies on the effect of pressure on diffusion at the MgO 410/[001] tilt grain boundary. Phys Rev B 64:134101–134108
8. McKenna KP, Shluger AL (2009) First-principles calculations of defects near a grain boundary in MgO. Phys Rev B 79:224116
9. Verma AK, Karki BB (2010) First-principles simulations of MgO tilt grain boundary: structure and vacancy formation at high pressure. Am Mineral 95:1035–1041
10. Vočadlo L, Wall A, Parker SC, Price GD (1995) Absolute ionic diffusion in MgO computer calculations via lattice dynamics. Phys Earth Planet Inter 88:193–210
11. Ita J, Cohen RE (1998) Diffusion in MgO at high pressure: implications for lower mantle rheology. Geophys Res Lett 25:1095–1098
12. Van Orman JA, Fei Y, Hauri EH, Wang J (2003) Diffusion in MgO at high pressures: constraints on deformation mechanisms and chemical transport at the core-mantle boundary. Geophys Res Lett 30:1056–1059
13. Niu K-Y, Yang J, Sun J, Du X-W (2010) One-step synthesis of MgO hollow nanospheres with blue emission. Nanotechnology 21:295604–295608
14. Yin Y, Rioux RM, Erdonmez CK, Hughes S, Somorjai GA, Alivisatos AP (2004) Formation of hollow nanocrystals through the nanoscale Kirkendall effect. Science 304:711–714
15. Pasquini L, Montone A, Callini E, Vittori Antisari M, Bonetti E (2011) Formation of hollow structures through diffusive phase transition across a membrane. Appl Phys Lett 99:021911
16. Mirabile Gattia D, Montone A, Pasquini L (2013) Microstructure and morphology changes in MgH_2/expanded natural graphite pellets upon hydrogen cycling. Int J Hydrogen Energy 38:1918–1924
17. Yang MH, Flynn CP (1994) Intrinsic diffusion properties of an oxide: MgO. Phys Rev Lett 73:1809–1812
18. Callini E, Pasquini L, Piscopiello E, Montone A, Vittori Antisari M, Bonetti E (2009) Hydrogen sorption in Pd-decorated Mg-MgO core-shell nanoparticles. Appl Phys Lett 94:221905
19. Keblinski P, Wolf D, Phillpot SR, Gleiter H (1997) Amorphous structure of grain boundaries and grain junctions in nanocrystalline silicon by molecular-dynamics simulation. Acta Mater 45:987–998
20. Keblinski P, Wolf D, Phillpot SR, Gleiter H (1997) Continuous thermodynamic-equilibriumglass transition in high-energy grain boundaries? Philos Mag Lett 76:143–152
21. Sangster MJL, Peckham G, Saunderson DH (1970) Lattice dynamics of magnesium oxide. J Phys C 3:1026–1036
22. Lewis GV, Catlow CRA (1985) Potential models for ionic oxides. J Phys C 18:1149–1161
23. Catlow CRA, Faux ID, Norgett MJ (1976) Shell and breathing shell model calculations for defect formation energies and volumes in magnesium oxide. J Phys C 9:419–429
24. Stoneham AM, Harding JH (1986) Interatomic potential in solid state chemistry. Annu Rev Phys Chem 37:53–80
25. Gale JD, Rohl AL (2003) The general utility lattice program. Mol Simulat 29:291–341
26. Smith W, Forester T (1996) DL_POLY_2.0: a general-purpose parallel molecular dynamics simulation package. J Mol Graph 14:136–141
27. Smith W (2006) Guest Editorial: DL_POLY-applications to molecular simulation II. Mol Simulat 32:933
28. DL_POLY code: www.ccp5.ac.uk/DL_POLY
29. Wolf D, Jaszcak JA (1992) Role of interface dislocations and surface steps in the work of adhesion. In: Wolf D, Yip S (eds) Materials interfaces: atomic-level structure and properties. Chapman & Hall, London, pp 662–690
30. Phillpot SR, Keblinski P, Wolf D, Cleri F (1999) Synthesis and characterization of a polycrystalline ionic thin film by large-scale molecular-dynamics simulation. Interface Sci 7:15–31
31. Saylor DM, Morawiec A, Rohrer GS (2003) Distribution of grain boundaries in magnesia as a function of five macroscopic parameters. Acta Mater 51:3663–3674
32. Mishin Y, Herzig C (1999) Grain boundary diffusion: recent progress and future research. Mater Sci Eng A260:55–71
33. Balluffi RW, Allen SM, Carter WC (2005) Kinetics of materials. John Wiley & Sons, Hoboken